 DOI: https://doi.org/10.5114/ceji.2023.129975

The role of murine M1 macrophages from different sources in unilateral ureteral obstruction

XINYU CUI[1], YAOWEN HU[1*], GENHONG ZHANG[2], LI ZHAO[1], TONG YE[2], QINGYAN ZHANG[3], JING LIU[3], CHUNMING JIANG[3], WEI ZHU[1,2,3,4]*

[1]Department of Nephrology, Nanjing Drum Tower Hospital, Clinical College of Traditional Chinese and Western Medicine, Nanjing University of Chinese Medicine, China
[2]Department of Nephrology, Nanjing Drum Tower Hospital, Clinical College of Jiangsu University, China
[3]Department of Nephrology, Nanjing Drum Tower Hospital, The Affiliated Hospital of Nanjing University Medical School, China
[4]Department of Nephrology, Nanjing Drum Tower Hospital, Clinical College of Nanjing Medical University, China

*These authors contributed equally to this work and should be considered co-first authors.

Abstract

Introduction: *The unilateral ureteral obstruction (UUO) model is the most extensively used model to investigate chronic renal fibrosis. Macrophages play a critical role in the UUO model. We aimed to analyze the phenotype of macrophages from different sources activated in vitro and explore the role of M1 macrophages from various sources in UUO.*

Material and methods: *C57BL/6 mice were randomly allocated to five different groups (n = 5 per group): the sham-operated control group, PBS-treated (UUO + PBS) group, bone marrow-derived M1 macrophage-treated (UUO + BM1) group, peritoneal M1 macrophage-treated (UUO + PM1) group, and splenic M1 macrophage-treated (UUO + SPM1) group. After M1 macrophages were injected into the tail vein of UUO-treated mice, renal fibrosis indexes were determined using HE, Masson staining, and α-SMA.*

Results: *Compared to those in the UUO + PBS group, the pathological changes were much more severe in the UUO + BM1, UUO + PM1, and UUO + SPM1 groups. Compared to that in the UUO + PBS group, UUO + BM1 group, and UUO + SPM1 group, the collagen area in the UUO + PM1 group was higher at post-UUO day 5 ($p < 0.01$). The expression of α-SMA in the UUO + PM1 group was higher than that in the UUO + PBS group, UUO + BM1 group, and UUO + SPM1group ($p < 0.001$).*

Conclusions: *The M1 macrophages cultured in vitro were reinjected into mice and aggravated kidney injury and fibrosis. Compared with BM1 and SPM1, PM1 demonstrated a stronger effect on inducing renal injury and fibrosis.*

Key words: *renal fibrosis, M1 macrophage, obstructive nephropathy, UUO.*

(Cent Eur J Immunol 2023; 48 (2): 81-91)

Introduction

Chronic kidney disease (CKD), a global public health issue, affects 8% to 16% of the world's population and causes substantial morbidity and mortality [1]. Renal fibrosis, which is characterized by fibroblast induction and extracellular matrix (ECM) production, is the terminal manifestation and the most prevalent irreversible mechanism in the progression to end-stage CKD [2]. Obstructive nephropathy is a vital factor in the pathogenesis of CKD induced by urinary flow dysfunction, which can cause kidney damage. The pathological process of renal injury can be prevented by surgery to relieve the obstruction. The pathological processes associated with renal obstruction are important during the pathogenesis of CKD [3]. The unilateral ureteral obstruction (UUO) model is the most extensively used model to investigate the etiology of acute renal inflammation and chronic renal fibrosis resulting from human ureteral blockage [4]. UUO affects the left ureter with high frequency. The kidney of the ligated ureter is usually referred to as the deterred kidney, and is affected by a series of critical processes, including the loss of renal epithelial cells, inflammation, and macrophage infiltration, all of which facilitate eventual fibrosis [5].

Macrophages pervade an extensive array of tissues, and their ability to control a large percentage of infections during early development, as well as their capacity to mount specific immune responses, attests to their im-

Correspondence: Wei Zhu, Nanjing Drum Tower Hospital, The Affiliated Hospital of Nanjing University Medical School, China, e-mail: zhuwell2018@163.com
Submitted: 07.01.2023, Accepted: 26.05.2023

portance. Macrophages are critical components of both innate and adaptive immunity [6]. Macrophages contribute to the preservation of homeostasis within renal tissue through the initiation of immunological reactions. Macrophages help maintain a stable environment in renal tissue by activating immune responses. Macrophages exhibit a variety of phenotypes under normal physiological conditions. They can be divided into two functional subcategories: classically activated macrophages (M1), which are defined by their antimicrobial and cytotoxic properties upon stimulation with endotoxin or interferon, and alternatively activated macrophages (M2), which are characterized by their anti-inflammatory and regulatory properties upon stimulation with Th2 cytokines and must be generated and function in balance to maintain homeostasis of the renal microenvironment [7, 8]. Macrophages play a critical role in UUO injury, and M1 macrophages can generate tumor necrosis factor α (TNF-α), which mediates proapoptotic signaling and renal tubular cell apoptosis following UUO [9].

Macrophages are frequently isolated from the bone marrow, spleen, and peritoneal cavity for research purposes [10]. It has been determined that the heterogeneity of macrophage populations accounts for distinct morphological differences among them. For macrophages to play diverse and adaptable roles in immune responses, they must exhibit diverse phenotypes. Consequently, there is a critical need to determine the phenotypic and practical variations among macrophages from distinct sources [6]. The aims of this study were to ascertain whether M1 macrophages derived from the bone marrow, spleen, and peritoneal cavity exacerbate renal injury and fibrosis in UUO mice, and to determine whether there are any differences in the extent of kidney damage caused by UUO among these sources. Macrophages were isolated from the bone marrow, spleen, and peritoneal cavity of mice. Macrophages were activated to form bone marrow-derived M1 macrophages (BM1), spleen-derived M1 macrophages (SPM1), and peritoneal M1 macrophages (PM1) by lipopolysaccharide and interferon γ, and we aimed to observe the outcomes of M1 macrophages from different sources in immunocompetent mice with UUO.

Material and methods

This study protocol was approved by the Experimental Animal Ethics Committee of Nanjing Hospital affiliated with Nanjing Medical University, approval number DWSY-22129258.

Animals

Adult male C57BL/6 mice, aged five weeks and weighing 20 g, were acquired from Nanjing Medical University (production license number: SYXK (Su2018-0008)) and kept in the Nanjing Drum Tower Experimental Animal Center (license number: SYXK (Su2019-0059)). All animal experiments were performed in accordance with the National Institutes of Health Guide for the Care and Use of Laboratory Animals, with the approval of the Experimental Animal Ethics Committee of Nanjing Medical University Affiliated Nanjing Hospital. All animals were housed in a controlled laboratory environment with a constant temperature of 22 ±2°C, a humidity level of 45 ±5%, a 12-hour day-night cycle, and free access to food and clean water. The animals were allowed to adapt for one week before surgery.

Experimental equipment

Jiangsu Zhenjiang Yihua Optical Instrument Co. offered the surgical microscope (Zhenjiang, China). The following items were purchased from Shanghai Pudong Jinhuan Medical Supplies Co.: microtweezers, microshears, and needle sutures (model 4-0, 7-0 round needle).

Methods

Mouse unilateral ureteral obstruction surgery

The mouse was placed supine on the operating table after being anesthetized intraperitoneally with 10% chloral hydrate (0.4 ml/100 g) (Boqiao Biotechnology Co., Nanjing, China). The hair was cut from the incision area with scissors. The surgical incision was made along the median of the lower abdomen. The peritoneal cavity was entered, the skin was cut, a midline laparotomy was performed, and the white line devoid of blood vessels was opened with tissue separation scissors. To expose the left ureter, the intestines were shifted to the right side of the abdomen using tweezers. The ureter was separated and ligated with forceps at two points with 7-0 silk thread (Shanghai Pudong Jinhuan Medical Supplies Co., Shanghai, China) and then cut between the two ligation points. The control mice that underwent a sham operation were subjected to abdominal laparotomy; however, the left ureter was not removed. The abdominal cavity was sutured layer by layer with a 4/0 black woven silk thread (Shanghai Pudong Jinhuan Medical Supplies Co., Shanghai, China) after washing with normal saline.

Experimental protocol for grouping and administration

Weight-matched mice were randomly assigned to five groups, as follows: (i) sham-operation group (sham, $n = 5$); (ii) UUO + PBS (phosphate-buffered saline) group ($n = 5$); (iii) BM1-treated group ($n = 5$); (iv) PM1-treated group ($n = 5$); (v) SPM1-treated group ($n = 8$). After being sorted, 1.0×10^6 BM1, PM1, and SPM1 cells were injected into the tail vein of each C57BL/6 J mouse in the UUO + BM1 group, UUO + PM1 group, and UUO + SPM1 group after UUO surgery. Mice in the UUO + PBS groups were treated with phosphate-buffered saline by the same method. Kidney samples were obtained from mice in each group on the 5th day after UUO.

Histology and morphometric evaluation

After 24 hours of fixation in 10% formalin solution, the kidney tissue was sliced into 3 μm paraffin sections. Staining with HE and Masson's trichrome was implemented based on conventional methods. Images were used to perform quantitative analysis of kidney tissue sections. The renal tubular injury score was measured by HE staining, with the observer blinded to the identity of the slides. The percentage of renal histological changes was calculated using the following semiquantitative scale to determine the degree of renal tubular necrosis: 0 represents normal, 1 represents mild damage (25% cortex), 2 represents moderate damage (25-50%), 3 represents severe damage (50-75%), and 4 represents damage to a considerable area (> 75%) [2]. Semiquantitative analysis of Masson's trichrome staining was performed using the proportion of collagen-positive regions. Collagen fibers (Masson trichrome, blue) were scored, and their positive area was calculated using a microscope eyepiece in ten bright visual fields (200×). The microscope (Nikon Eclipse E100) and digital camera (NIKON DS-U3) were purchased from Japan.

Kidney immunohistochemistry

Paraffin-embedded kidney sections (4 mm thick) were used to determine the expression level of α-smooth muscle actin (α-SMA) in the kidney. The dewaxed tissue sections were incubated with 3% hydrogen peroxide in water to eliminate endogenous peroxidase. After overnight incubation at 4°C with the primary antibody, the slides were incubated for 30 minutes at 37°C with the biotinylated secondary antibody. Following DAB staining, the sections were restrained with hematoxylin and dehydrated, and cover slides were applied to seal them [5]. A Nikon Eclipse E100 microscope was used in conjunction with a Nikon DS-U3 digital camera to capture high-resolution images of the stained tissue samples. The results were assessed quantitatively using the ImageJ system, and ten high-power fields (400× magnification) were analyzed separately for each immunohistochemical reaction in renal tissue.

Isolation and polarization of macrophages from bone marrow, spleen and peritoneal cavity

Bone marrow macrophages were isolated and purified as described previously [11]. The bone marrow from mouse femurs was flushed and washed through a 70 μm nylon mesh, and the erythrocytes were lysed in lysis buffer. The obtained cells were cultured under 5% CO_2 at 37°C. The adherent cells were rinsed and immersed in fresh culture medium after 2 to 3 days. For M0 macrophages (BM0), adherent cells were washed and cultured for 7 days [12]. These cells were then cultured for 48 hours with 100 ng/ml lipopolysaccharide (Sigma), and 50 ng/ml interferon γ (R&D). We obtained M1 macrophages (BM1) [13]. Trypsin (0.25%) was applied to harvest the cells.

Spleen M0 macrophages (SPM0) were isolated and purified as described previously [14]. The spleen was removed from the peritoneal cavity and filtered with a 40-micrometer nylon filter. For elimination of red blood cells, red cell lysis buffer was utilized. The cells were cultured under 5% CO_2 at 37°C. After 40 min, the culture supernatant was discarded, and the adherent cells were rinsed three times. The adherent spleen-derived macrophages were cultured for 48 h with normal medium for M0 cells, with 100 ng/ml LPS (Sigma)/IFN-γ 50 ng/ml (R&D) for M1 cells (SPM1). Trypsin (0.25%) was used to harvest the cells.

Peritoneal macrophages isolated from C57BL/6 mice (PM0) were polarized to the M1 phenotype using a previously described method [15]. Peritoneal M0 macrophages were polarized to the M1 phenotype (PM1) after treatment with 100 ng/ml LPS (Sigma) in the presence of 50 ng/ml IFN-γ (R&D) for 48 h. Trypsin (0.25%) was applied to harvest the cells.

Macrophage labeling and adoptive transfer to C57BL/6 mice

Bone marrow, spleen, and peritoneal macrophages were extracted from 4-week-old male C57BL/6 mice and stimulated with LPS and IFN-γ to promote M1 differentiation. The resulting bone marrow-derived M1 macrophages, spleen-derived M1 macrophages, and peritoneal M1 macrophages were labeled with 3,3′-dioctadecyloxacarbocyanine perchlorate (DIO; Beyotime) for *in vivo* studies. The labeled macrophages were washed three times with PBS. Kidneys were collected on the five days following macrophage infusion to examine the phenotypes of the injected macrophages. Separation of kidney mononuclear cells by sucrose gradient separation and staining with PE-conjugated anti-mouse CD11b were performed. Flow cytometry analysis of exogenous renal macrophages ($CD11b^+DiO^-$) and transplanted macrophages ($CD11b^+DiO^+$) was performed.

Flow cytometry analysis

We resuspended the macrophages in auto MACS Rinsing Solution. Nonspecific Ab binding was blocked using an Fc blocking Ab, and the purity of isolated macrophages was determined by staining with APC-conjugated anti-mouse F4/80 (BioLegend). The surface markers of macrophages were evaluated using PE/CY7-conjugated anti-mouse CD86 (Thermo). To stain CD206 intracellularly, macrophages were fixed and incubated with PE-conjugated anti-mouse CD206. Flow cytometry was performed using a FACSCalibur cytometer (BD Biosciences) and analyzed with FlowJo software.

Real-time PCR analysis

RNA was extracted using RNAiso Plus (TaKaRa, Japan) as directed by the manufacturer; the first strand of cDNA was synthesized from total RNA using the Prime Script RT kit and gDNA Eraser (Perfect Real Time)

(TaKaRa, Japan) as directed by the manufacturer. Then, real-time PCR was performed using TB Green Premix Ex Taq II (Tli RNaseH Plus) (TaKaRa, Japan). The PCR mixture, which included primers, cDNA, and SYBR green master mix, was run in real time on a Corbett Rotorgene 6000 real-time Thermocycler. The following primers (forward and reverse) were applied: IL-12, 5′-CAATCACGCTACCTCCTCTTTT-3′ and 5′-CAGCAGTGCAGGAATAATGTTTC-3′; TNF-α, 5′-CCTGTAGCCCACGTCGTAG-3′ and 5′-GGGAGTAGACAAGGTACAACCC-3′; inducible nitric oxide synthase (INOS), 5′-CTTGGAGCGAGTTGTGGATTGTC-3′ and 5′-ATTGTACTCTGAGGGCTGACACA-3′; IL-10, 5′-AGCCGGGAAGACAATAACTGC-3′ and 5′-AACCCAAGTAACCCTTAAAGTCCTG-3′; CD206, 5′-CTCTGTTCAGCTATTGGACGC-3′ and 5′-TGGCACTCCCAAACATAATTTGA-3′; and glyceraldehyde-3-phosphate dehydrogenase (GAPDH), 5′-CAAGGTCATCCATGACAACTTTG-3′ and 5′-GTCCACCACCCTGTTGCTGTAG-3′. GraphPad Prism 8.0 was used for statistical analysis.

Phagocytic capacity assay of spleen-derived M1 macrophages, bone marrow-derived M1 macrophages, and peritoneal M1 macrophages

The pinocytic activity of macrophages was ascertained using the neutral red uptake assay. For 48 hours, macrophages (5×10^3 cells/well) were treated with lipopolysaccharide (LPS; 100 ng/ml; Sigma) and interferon (IFN; 50 ng/ml; R&D). The cell culture medium was removed, and 100 µl/well of 0.075% neutral red was added. Cells, which were kept for 30 minutes at 37°C, were washed with PBS three times. Each well was cultured at 4°C for another 30 minutes with a cell lysate (150 µl/well) containing acetic acid and ethanol (volume ratio of 1 : 1). The absorbance was determined at 570 nm using a Bio-Rad model 680 Microplate Reader (Pennsylvania, USA).

Statistical analysis

The statistical analysis software SPSS 22.0 and GraphPad Instant 8.0 were used. Nonparametric tests were used for comparisons between two groups, and for comparisons among multiple groups. One-way analysis of variance (ANOVA) followed by Tukey's multiple comparison test was used as appropriate. Statistical significance was defined as a p value less than 0.05. Data are expressed as the median.

Results

Morphological differences between spleen-derived M1 macrophages, bone marrow-derived M1 macrophages, and peritoneal M1 macrophages

The morphology of macrophages stimulated with lipopolysaccharide (LPS; 100 ng/ml; Sigma) and interferon γ (IFN-γ; 50 ng/ml; R&D) varied. We found that BM1 macrophages were fusiform, and their pseudopods gradually became shorter and rounder than those of BM0 macrophages. Most PM1 macrophages were round in comparison to PM0 macrophages. BM1 macrophages had a longer spindle profile than SPM1 and PM1 macrophages (Fig. 1).

Phagocytic capacity of spleen-derived M1 macrophages, bone marrow-derived M1 macrophages, and peritoneal M1 macrophages

The phagocytic capacity of these three groups of macrophages was assessed. Macrophages derived from the three different sources absorbed a significant amount of neutral red. Compared to M0 macrophages (resting macrophages), M1 macrophages absorbed less neutral red. We found that BM1 and PM1 macrophages had a greater capacity for phagocytosis than SPM1 macrophages (Fig. 1).

Macrophages isolated from the bone marrow, spleen and peritoneal cavity can differentiate into the M1 phenotype

Macrophages exist in a variety of activation states to fulfill their various physiological functions. We compared the activation states of M1 macrophages based on the expression and secretion of markers and related factors. The expression of F4/80, CD206, and CD86 was examined by flow cytometry analysis. More than 90% of these three types of M1 macrophages were F4/80+, and they were all $CD86^+CD206^-$ (Fig. 2). We assessed the relative mRNA levels of TNF-α, inducible nitric oxide synthase (INOS), CD206, IL-12, IL-10, and Arg-1 when the macrophages were stimulated with IFN-γ and LPS for 48 h to differentiate the M1 state. In comparison with BM0, SPM0, and PM0 macrophages, SPM1, BM1, and PM1 macrophages expressed high levels of INOS, TNF-α, and IL-12. Therefore, the three distinct subtypes of macrophages are capable of polarizing into the M1 phenotypic state according to our findings. The three different sources were analyzed to determine the differences between the M1 states. The comparative data showed that BM1 and PM1 macrophages expressed higher mRNA levels of INOS under the M1 condition ($p < 0.0001$). Compared to BM1 macrophages and SPM1, PM1 macrophages expressed higher mRNA levels of IL-10. PM1 macrophages also expressed higher levels of IL-12 and TNF than BM1 and SPM1 macrophages ($p < 0.0001$). There were no differences in the ability of the three macrophages to express CD206 mRNA (Fig. 2).

M1 macrophage reperfusion aggravates renal injury in UUO-treated mice

HE staining showed that the intratubular space increased substantially, tubulointerstitial cells infiltrated, renal tubular epithelial cells were partially exfoliated,

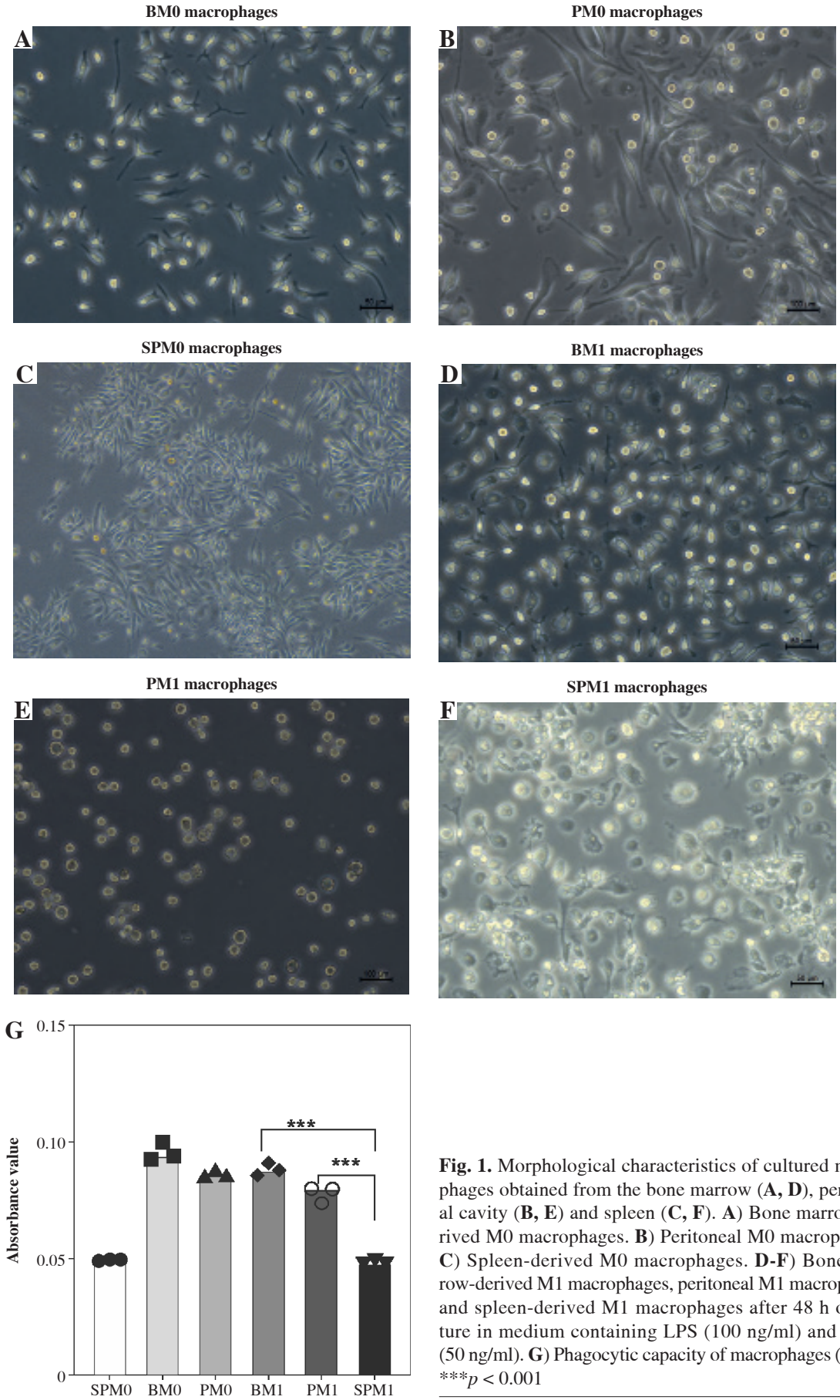

Fig. 1. Morphological characteristics of cultured macrophages obtained from the bone marrow (**A, D**), peritoneal cavity (**B, E**) and spleen (**C, F**). **A**) Bone marrow-derived M0 macrophages. **B**) Peritoneal M0 macrophages. **C**) Spleen-derived M0 macrophages. **D-F**) Bone marrow-derived M1 macrophages, peritoneal M1 macrophages and spleen-derived M1 macrophages after 48 h of culture in medium containing LPS (100 ng/ml) and IFN-γ (50 ng/ml). **G**) Phagocytic capacity of macrophages ($n = 3$). ***$p < 0.001$

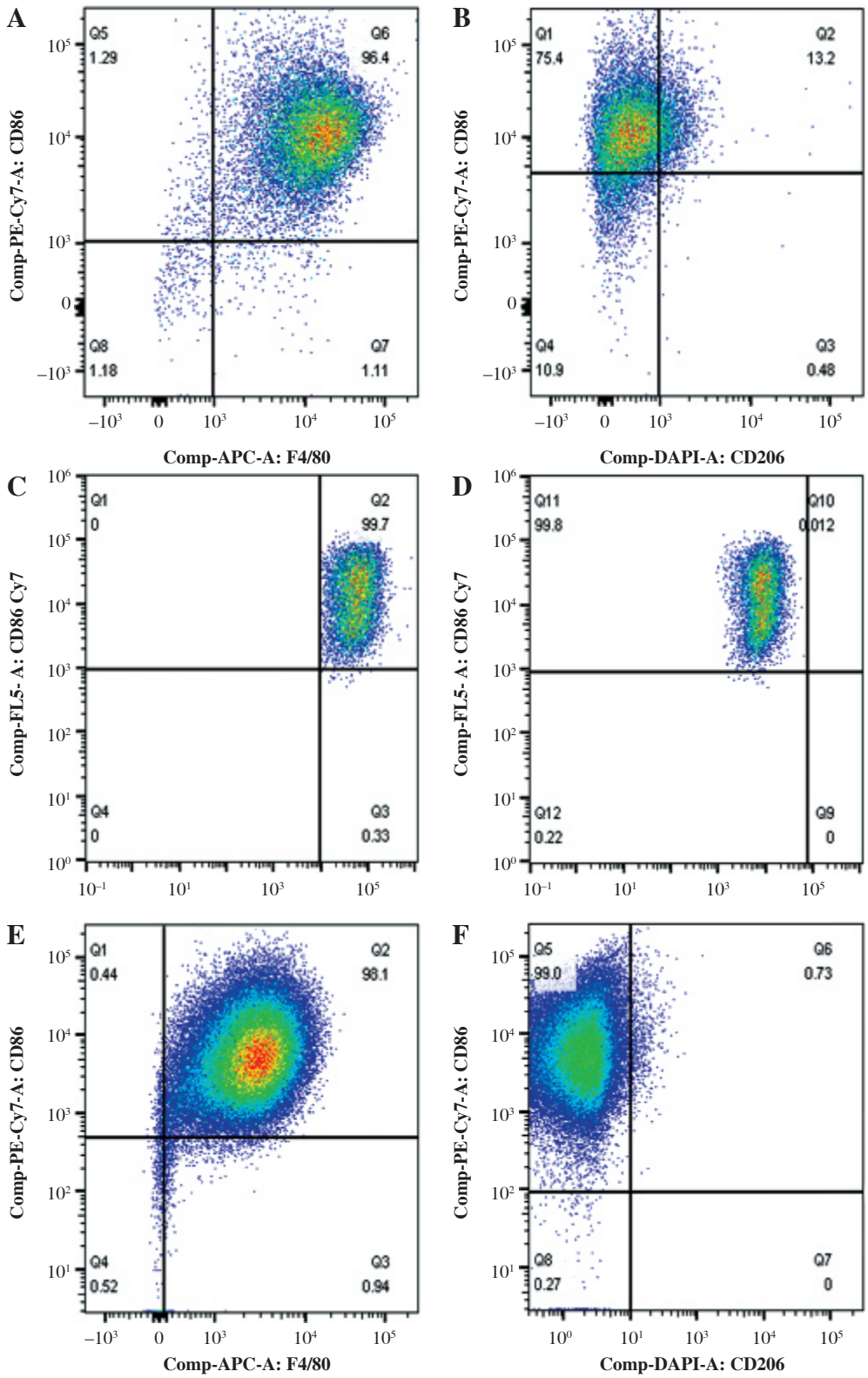

Fig. 2. Expression of F4/80, CD86, and CD206 in M0 and M1 macrophages. **A**) Expression of F4/80 and CD86 in bone marrow-derived M1 macrophages. **B**) Expression of CD206 and CD86 in bone marrow-derived M1 macrophages. **C**) Expression of F4/80 and CD86 in spleen-derived M1 macrophages. **D**) Expression of CD206 and CD86 in spleen-derived M1 macrophages. **E**) Expression of F4/80 and CD86 in peritoneal M1 macrophages. **F**) Expression of CD206 and CD86 in peritoneal M1 macrophages

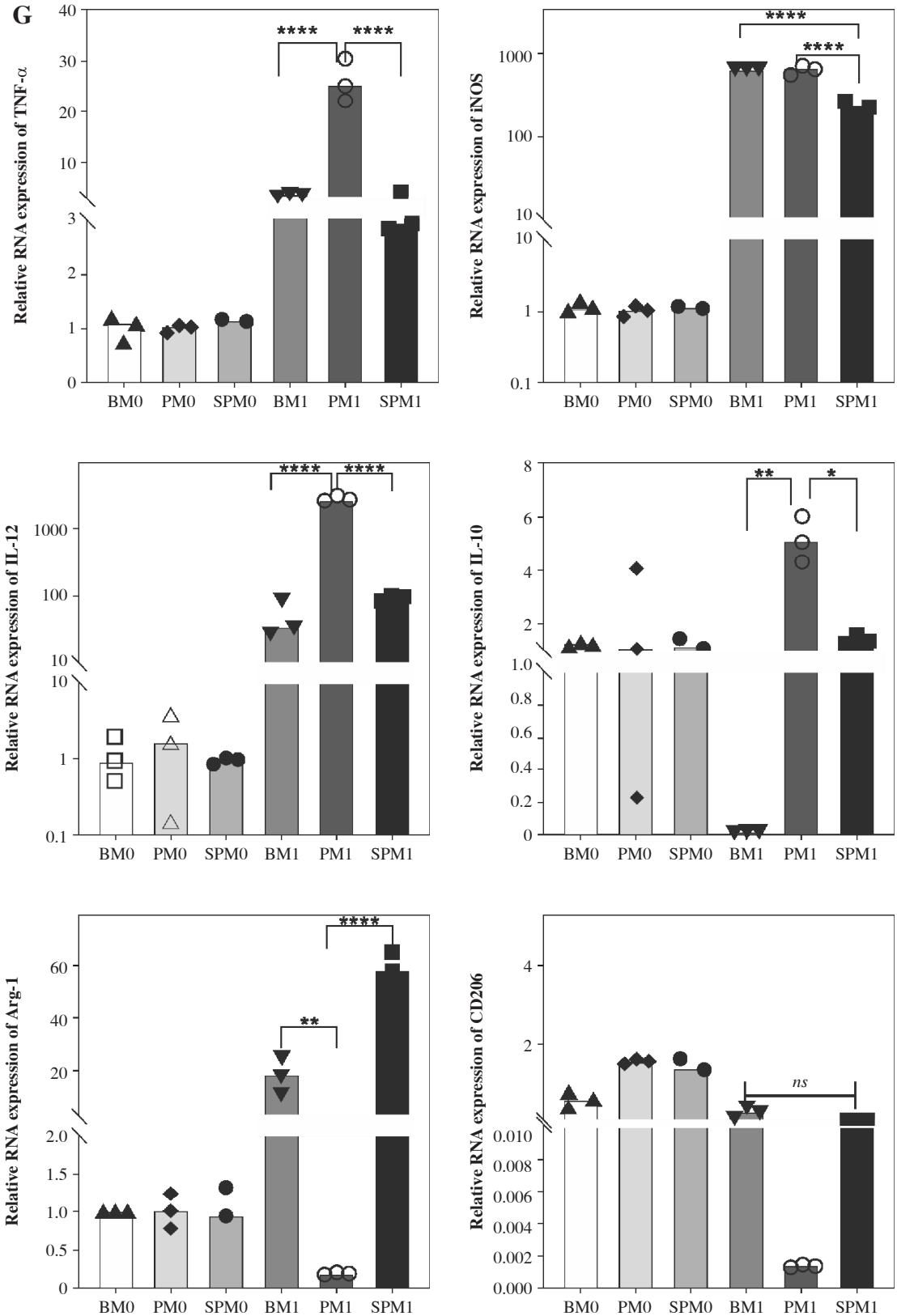

Fig. 2. Cont. **G**) Profiles of cytokine mRNA expression in three kinds of M0 and M1 macrophages. mRNA expression of TNF-α, INOS, CD206, IL-12, IL-10, and Arg-1 was measured by quantitative PCR relative to the control for each experiment ($n = 3$). Data represent the median. *$p < 0.05$, **$p < 0.01$, ****$p < 0.0001$

and the tubular lumen dilated. The tubular necrosis score of kidneys in the UUO + PM1 groups was higher than that in the UUO + BM1 and UUO + SPM1 groups (Fig. 3).

The sham-operated group had no obvious blue-stained area after Masson staining, whereas there were obvious blue areas in the UUO + PBS group and the UUO + BM1, UUO + PM1, UUO + SPM1 groups, which were mainly distributed in the renal interstitium. The UUO + PM1 group had more blue areas than the UUO + PBS group. The collagen area ratios in the UUO + PM1 group were higher than those in the UUO + PBS group. The proportion of the collagen area in the kidneys in the sham, UUO + PBS, UUO + BM1, UUO + PM1, and UUO + SPM1 groups was 14.49 ±4.26%, 29.46 ±1.35%, 28.87 ±2.91%, 50.30 ±9.83%, and 32.93 ±5.87%, respectively (Fig. 3).

Immunohistochemical staining demonstrated that the expression of α-SMA was lower in the sham operation group, particularly in the walls of small blood vessels and around glomeruli and renal tubules. The expression of α-SMA in the UUO + PM1 groups was higher than that in the UUO + PBS group and was mainly distributed in renal tubulointerstitial areas. The average absorbance of α-SMA in the UUO + PM1 and UUO + SPM1 groups was higher than that in the UUO + PBS group. The expression of α-SMA in the kidneys of the sham, UUO + PBS, UUO + BM1, UUO + PM1, and UUO + SPM1 groups was 0.1873 ±0.018, 0.2813 ±0.023, 0.3647 ±0.032, 0.4323 ±0.022, and 0.344 ±0.025, respectively (Fig. 3).

Discussion

Macrophages play an important role in the genesis and progression of renal inflammation and fibrosis [16]. Macrophage populations are considerably diverse among tissues. The functional differences of macrophages in different tissues still need to be explored. In the present study, we investigated the effects of three different sources of M1 macrophages on kidney injury. We found that although macrophages from bone marrow, spleen, and the peritoneal cavity could all differentiate into the M1 phenotype, their morphology, phenotype, and function were slightly different. PM1 macrophages expressed higher levels of TNF-α than BM1 and SPM1 macrophages. Therefore, the effects of BM1, SPM 1 and PM1 on UUO renal injury and fibrosis are not completely consistent. Compared with BM1 and SPM1, PM1 has a stronger effect on inducing renal injury and fibrosis.

Macrophage subsets include typical activated or inflammatory (M1) macrophages and alternately activated or anti-inflammatory (M2) macrophages. M1 macrophages produce interleukin 12 (IL-12) and inducible nitric oxide synthase (INOS), which can promote inflammation and chemotaxis, and induce matrix decomposition [17]. Macrophage populations are diverse, and they are considerably diverse among tissues. Even with the same phenotype, the effects of macrophages from different sources may be different [18]. This study compared the morphology, phagocytic ability, and phenotypes of M1 macrophages from three different sources. It was found that BM1 macrophages had a more elongated spindle shape than SPM1 and PM1 macrophages. In addition to morphology, the phagocytic ability of macrophages was evaluated. BM1 and PM1 macrophages have been proven to have high phagocytic ability.

The macrophage lines RAW264.7, P388D1, and U937 can be applied to research macrophages [19, 20]; constant culture of these cell lines, however, may lead to gene loss and a reduction in macrophage immune function. As a result, primary culture bone marrow macrophages, spleen macrophages, and peritoneal macrophages have been used in the majority of experimental research. In the bone marrow, monocytes from macrophage and dendritic cell progenitor-derived pro-monocyte precursors infiltrate to form tissue macrophages, and the precursors can be differentiated into macrophages *in vitro*. The spleen is the main immune organ and contains a large number of immune cells, which can be obtained as a single cell suspension, and macrophages can be acquired by adhesion and purification. The peritoneal cavity typically contains primary macrophages from mice. Macrophages accounted for 35% of the cells in the peritoneal cavity [21]. Peritoneal macrophages are more readily available than bone marrow and spleen macrophages. At present, most macrophages used in cell therapy are derived from bone marrow [22] and spleen [23], and macrophages from the peritoneal cavity are rarely used in cell therapy. Our research demonstrated that the isolated macrophages are all capable of polarizing into M1 phenotypes, implying that macrophage plasticity may aid in disease control and therapy.

Obstructive nephropathy is a prevalent clinical condition with irreversible long-term consequences, such as renal fibrosis. UUO is an excellent model for the study of obstructive nephropathy [24]. Macrophages were recruited into the renal interstitium in the UUO model. This migration begins on the first day of UUO and continues throughout the course of progression. As the first line of defense, M1 macrophages enter the UUO renal cortex [25]. M0 macrophages can be polarized to M1 macrophages by pathogen-related molecular patterns (PAMPs), such as lipopolysaccharides (LPS). These cells secrete a series of proinflammatory factors (including IL-6, IL-12, and TNF-α), activated oxygen species, and nitric oxide (NO), which promote inflammation [16]. The results showed that adoptive transfer of BM1, PM1 and SPM1 macrophages could significantly increase renal inflammatory cell infiltration, partial exfoliation of renal tubular epithelial cells and lumen dilatation in UUO. In the late stage of UUO, M2 macrophages are predominant in UUO-treated kidneys, which promote renal fibrosis [26]. According to Jiong Cui's study, complement C3 exacerbates renal interstitial fibrosis by facilitating macrophage M1 polarization, promoting proinflammatory cytokine expression [27].

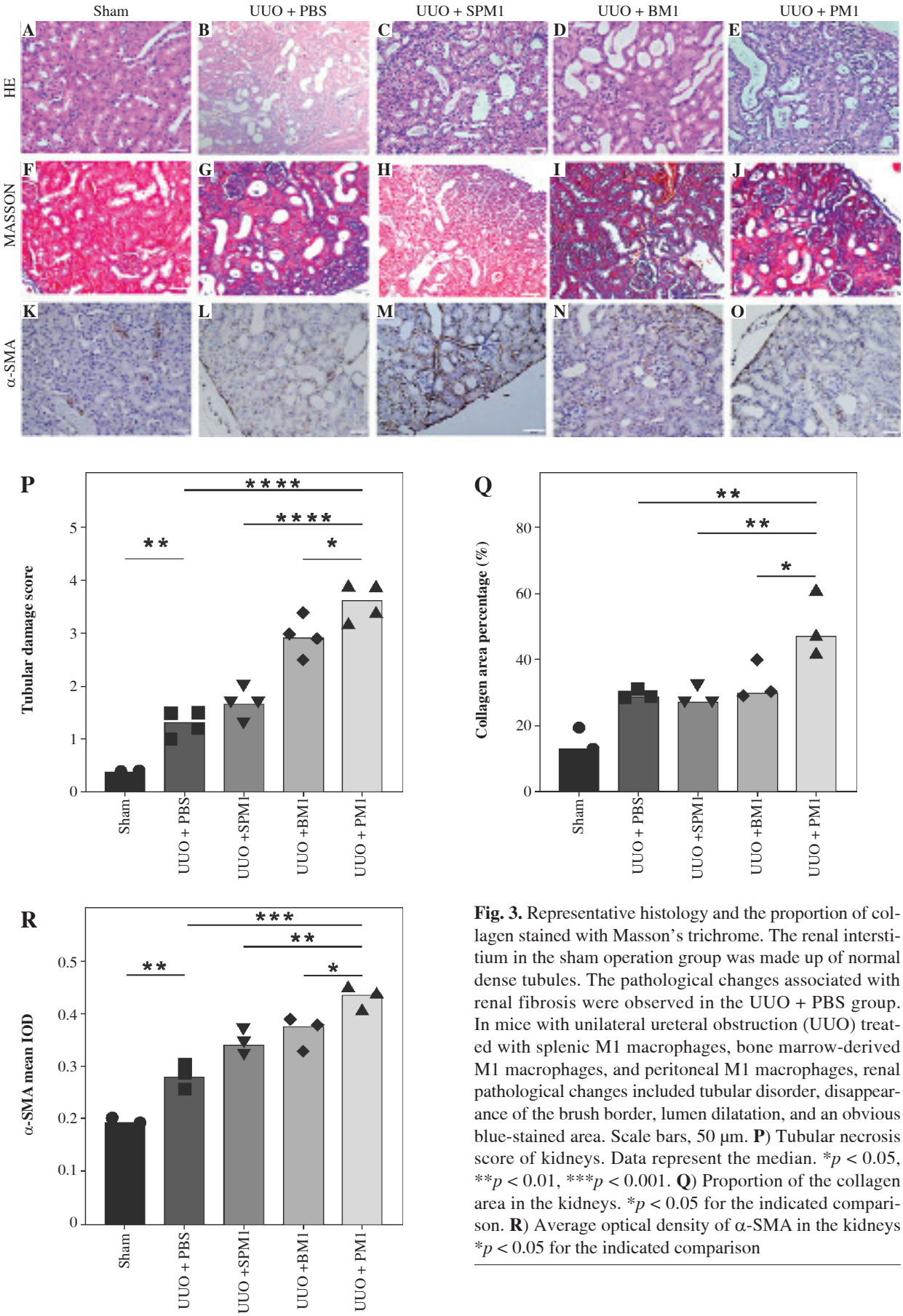

Fig. 3. Representative histology and the proportion of collagen stained with Masson's trichrome. The renal interstitium in the sham operation group was made up of normal dense tubules. The pathological changes associated with renal fibrosis were observed in the UUO + PBS group. In mice with unilateral ureteral obstruction (UUO) treated with splenic M1 macrophages, bone marrow-derived M1 macrophages, and peritoneal M1 macrophages, renal pathological changes included tubular disorder, disappearance of the brush border, lumen dilatation, and an obvious blue-stained area. Scale bars, 50 μm. **P**) Tubular necrosis score of kidneys. Data represent the median. *$p < 0.05$, **$p < 0.01$, ***$p < 0.001$. **Q**) Proportion of the collagen area in the kidneys. *$p < 0.05$ for the indicated comparison. **R**) Average optical density of α-SMA in the kidneys *$p < 0.05$ for the indicated comparison

However, the role of BM1, PM1 and SPM1 in fibrosis in the mouse UUO model is still unclear. We found that many pathological markers of renal fibrosis, including the collagen content, and α-SMA expression in the kidneys, were considerably higher in the UUO + PM1 and UUO + SPM1 groups compared with the UUO + PBS group.

Tumor necrosis factor α can modulate the progression of acute kidney disease and CKD and alter the severity of renal injury [28]. According to Jian Ping Sheng's study, TNF-α is indispensable for the development of fibrosis [29]. Our research demonstrated that PM1 macrophages expressed higher levels of TNF-α than BM1 and SPM1 macrophages. This result may be the reason why the renal tubular injury score, α-SMA integrated optical density (IOD) value and fibrosis score of the UUO + PM1 group are higher than those of the UUO + BM1 and UUO + SPM1 groups.

Although our study demonstrates that different sources of M1 have different effects on UUO 5-day renal interstitial inflammation and fibrosis, there are limitations. First, we only observed the effect of M1 on the early stage of UUO. We should further observe the effect of three different sources of M1 macrophages on the UUO model for 7 days and 14 days and whether they will aggravate UUO fibrosis as in the early stage. Second, according to Bing Shen's research, in the late stage of UUO, M2 macrophages are mainly found [26]. In future studies, M2 macrophages can be reinfused to observe their impact on the UUO model. Finally, studies have shown that JAK/STAT1 is involved in liver fibrosis caused by M1 macrophages [30], and whether M1 macrophages play a fibrotic role in the kidney through JAK/STAT1 needs further study.

Conclusions

In conclusion, we provide evidence that M1 macrophages can aggravate renal structural and functional damage in UUO. In a comparison of macrophages from three different sources, peritoneal macrophages had stronger inflammatory effects to some extent. The mechanism by which interstitial inflammation is greatly enhanced by M1 macrophages obtained from the peritoneum needs to be further explored.

Funding

This study was funded by Nanjing Health Youth Talent (QRX17045).

The authors declare no conflict of interest.

References

1. Santana Machado T, Cerini C, Burtey S (2019): Emerging roles of aryl hydrocarbon receptors in the altered clearance of drugs during chronic kidney disease. Toxins (Basel) 11: 209.
2. Chen W, Yuan H, Cao W, et al. (2019): Blocking interleukin-6 trans-signaling protects against renal fibrosis by suppressing STAT3 activation. Theranostics 9: 3980-3991.
3. Lucarelli G, Ditonno P, Bettocchi C, et al. (2013): Delayed relief of ureteral obstruction is implicated in the long-term development of renal damage and arterial hypertension in patients with unilateral ureteral injury. J Urol 189: 960-965.
4. Kim JI, Noh MR, Yoon GE, et al. (2021): IDH2 gene deficiency accelerates unilateral ureteral obstruction-induced kidney inflammation through oxidative stress and activation of macrophages. Korean J Physiol Pharmacol 25: 139-146.
5. Bai Y, Wang W, Yin P, et al. (2020): Ruxolitinib alleviates renal interstitial fibrosis in UUO mice. Int J Biol Sci 16: 194-203.
6. Wang C, Yu X, Cao Q, et al. (2013): Characterization of murine macrophages from bone marrow, spleen and peritoneum. BMC Immunol 14: 6.
7. Cao Q, Wang Y, Zheng D, et al. (2010): IL-10/TGF-beta-modified macrophages induce regulatory T cells and protect against adriamycin nephrosis. J Am Soc Nephrol 2010; 21: 933-942.
8. Liao Y, Tan RZ, Li JC, et al. (2020): Isoliquiritigenin attenuates UUO-induced renal inflammation and fibrosis by inhibiting Mincle/Syk/NF-kappa B signaling pathway. Drug Des Devel Ther 14: 1455-1468.
9. Chevalier RL, Forbes MS, Thornhill BA (2009): Ureteral obstruction as a model of renal interstitial fibrosis and obstructive nephropathy. Kidney Int 75: 1145-1152.
10. Zhao YL, Tian PX, Han F, et al. (2017): Comparison of the characteristics of macrophages derived from murine spleen, peritoneal cavity, and bone marrow. J Zhejiang Univ Sci B 2017; 18: 1055-1063.
11. Weischenfeldt J, Porse B (2008): Bone marrow-derived macrophages (BMM): Isolation and applications. CSH Protoc 2008: pdb.prot5080.
12. Pineda-Torra I, Gage M, de Juan A, Pello OM. Isolation, culture, and polarization of murine bone marrow-derived and peritoneal macrophages. Methods Mol Biol 2015; 1339: 101-109.
13. Huang X, Li Y, Fu M, Xin HB (2018): Polarizing macrophages in vitro. Methods Mol Biol 1784: 119-126.
14. Lu J, Cao Q, Zheng D, et al. (2013): Discrete functions of M2a and M2c macrophage subsets determine their relative efficacy in treating chronic kidney disease. Kidney Int 84: 745-755.
15. Jia X, Li X, Shen Y, et al. (2016): MiR-16 regulates mouse peritoneal macrophage polarization and affects T-cell activation. J Cell Mol Med 20: 1898-1907.
16. Wang X, Chen J, Xu J, et al. (2021): The role of macrophages in kidney fibrosis. Front Physiol 12: 705838.
17. Italiani P, Boraschi D (2014): From monocytes to M1/M2 macrophages: Phenotypical vs. functional differentiation. Front Immunol 2014; 5: 514.
18. Locati M, Curtale G, Mantovani A (2020): Diversity, mechanisms, and significance of macrophage plasticity. Annu Rev Pathol 2020; 15: 123-147.
19. Back YS, Haas S, Hackstein H, et al. (2009): Identification of novel transcriptional regulators involved in macrophage differentiation and activation in U937 cells. BMC Immunol 10: 18.
20. Goodrum KJ (1987): Complement component C3 secretion by mouse macrophage-like cell lines. J Leukoc Biol 41: 295-301.
21. Zhao YL, Tian PX, Han F, et al. (2017): Comparison of the characteristics of macrophages derived from murine

spleen, peritoneal cavity, and bone marrow. J Zhejiang Univ Sci B 18: 1055-1063.
22. Starkey Lewis P, Campana L, Aleksieva N, et al. (2020): Alternatively activated macrophages promote resolution of necrosis following acute liver injury. J Hepatol 73: 349-360.
23. Tang L, Zhang H, Wang C, et al. (2017): M2A and M2C macrophage subsets ameliorate inflammation and fibroproliferation in acute lung injury through interleukin 10 pathway. Shock 48: 119-129.
24. Wang J, Ge S, Wang Y, et al. (2021): Puerarin alleviates UUO-induced inflammation and fibrosis by regulating the NF-kappaB P65/STAT3 and TGFbeta1/Smads signaling pathways. Drug Des Devel Ther 15: 3697-3708.
25. Martínez-Klimova E, Aparicio-Trejo OE, Tapia E, Pedraza-Chaverri J (2019): Unilateral ureteral obstruction as a model to investigate fibrosis-attenuating treatments. Biomolecules 9: 141.
26. Shen B, Liu X, Fan Y, Qiu J (2014): Macrophages regulate renal fibrosis through modulating TGFβ superfamily signaling. Inflammation 37: 2076-2084.
27. Cui J, Wu X, Song Y, et al. (2019): Complement C3 exacerbates renal interstitial fibrosis by facilitating the M1 macrophage phenotype in a mouse model of unilateral ureteral obstruction. Am J Physiol Renal Physiol 317: F1171-F1182.
28. Wen Y, Lu X, Ren J, et al. (2019): KLF4 in macrophages attenuates TNF-mediated kidney injury and fibrosis. J Am Soc Nephrol 30: 1925-1938.
29. Sheng J, Zhang B, Chen Y, Yu F (2020): Capsaicin attenuates liver fibrosis by targeting Notch signaling to inhibit TNF-α secretion from M1 macrophages. Immunopharmacol Immunotoxicol 42: 556-563.
30. Zhang J, Liu Y, Chen H, et al. (2022): MyD88 in hepatic stellate cells enhances liver fibrosis via promoting macrophage M1 polarization. Cell Death Dis 13: 411.